Error Mitigation in UWB-Based Positioning Systems Using an Adapted Tree Approach

M.M Saberi[1], M. Azimi[2], M.M Shahnavaz[3], S. Ebadollahi[4]*, H. Najafi[5], and M.A Sobati[6]

[1] School of Electrical Engineering, Iran University of Science and Technology, Tehran, Iran (e-mail: saberi_mo@elec.iust.ac.ir).
[2] School of Electrical Engineering, Iran University of Science and Technology, Tehran, Iran (e-mail: Mohammad_azimi@elec.iust.ac.ir).
[3] School of Electrical Engineering, Iran University of Science and Technology, Tehran, Iran (e-mail: m.m.Shahnavaz@gmail.com).
[4] School of Electrical Engineering, Iran University of Science and Technology, Tehran, Iran (e-mail: s_ebadollahi@iust.ac.ir).
[5] Farayand Sabz Engineering Company, No.117, Somaye Street, 158176-8511 Tehran, Iran (e-mail: hrnajafi@xthermo.com).
[6] School of Chemical Engineering, Iran University of Science and Technology, Tehran, Iran (e-mail: Sobati@iust.ac.ir).

*Corresponding Author

Received 17 June 2023 Received in revised form 15 Feb. 2024 Accepted 26 May 2024

Type of Article: Research paper

***Abstract*—This paper addresses the challenge of mitigating positioning errors in Ultra-Wide Band (UWB) networks. We propose an adapted tree approach that compensates for error effects, leading to improved accuracy in both Line-of-Sight (LOS) and Non-Line-of-Sight (NLOS) environments. The ranging errors are classified into two types, LOS and NLOS condition errors, and the adapted tree approach starts with splitting the study based on the presence of these conditions. The ranging error values are studied in different distances and intervals are identified based on the standard deviation error criterion. The positioning results are presented and analyzed, showing that utilizing the adapted tree leads to an average error mitigation of about 53.4 cm in the LOS condition and about 133 cm in the NLOS condition. The results demonstrate the effectiveness of the adapted tree approach in error mitigation for both LOS and NLOS conditions. Furthermore, the EKF estimation method is found to be the most accurate estimator. Finally, the proposed approach is applied on a moving tag, achieving an accuracy of about 20.8 cm for LOS and 24.1 cm for NLOS conditions through the EKF method.**

***Keywords*: Indoor Positioning Systems, Real-Time Locating Systems, Error Mitigation, Extended Kalman Filter.**

I. INTRODUCTION

THE Internet of Things (IoT) has gained increasing attention, and its potential continues to be discovered over time. IoT is the idea of connecting objects to enable communication among them and with users [1]. Positioning can be broadly classified into global and local modes, with local positioning being a common use case for IoT. Despite the numerous benefits of local positioning, it faces various challenges, such as accuracy and stability.

Recent approaches for solving the positioning problem can be categorized into two different methods: vision-based and beacon-based [2]. The latter includes various options, such as ultrasonic ranging, optical positioning, infrared radiation, and Radio Frequency (RF) [3]. Among the available RF-based technologies, UWB technology stands out due to its desirable features, including high accuracy, resistance to noise, no interference with other radio systems, wall penetration, and high-speed transmission [3-5].

UWB works by using fixed and known anchor nodes to signal with mobile objects, called tags [6]. Various algorithms are available for UWB, including Received Signal Strength Indication (RSSI) [7], Angle of Arrival (AOA), and time-based algorithms such as Time of Arrival (TOA), Time Difference of Arrival (TDOA), and Two-

Way Ranging (TWR) [4, 8]. However, path loss is an issue with UWB, and the RSSI algorithm's effectiveness may decrease due to signal strength reduction during travel. Thus, the time-based algorithms would be the best option for higher accuracy [4, 7]. In [9], a UWB error map-building method is proposed along with an adapted error map-based particle filter to enhance the accuracy of UWB positioning.

The TWR algorithm is preferred among other available technologies due to the challenges in TOA/TDOA clock synchronization [7, 8]. TWR estimates the Time of Flight (TOF) of the signal and does not require clock synchronization, thereby using periods instead of timestamps [10, 11].

However, one of the main challenges in UWB systems is the requirement for LOS path between nodes, which can be obstructed in indoor scenarios, particularly in dense multipath propagation environments. In the absence of the LOS path, NLOS paths, such as penetrated, reflected, diffracted, or scattered paths [12], can be used by the transmitted signal from a tag to reach the anchors. To minimize inaccuracies caused by these factors, various works have been proposed in [10, 12-14].

For example, a self-training method is introduced in [15], which leverages integrating maps, inertial sensors, and UWB measurements to mitigate errors. In [16], tracking motion dynamics and visibility conditions of the UWB antennas are jointly used to mitigate positioning errors. Additionally, a through-the-wall ranging model is developed in [17] to mitigate ranging errors, and a novel algorithm is proposed in [18, 19] for mixed LOS-NLOS conditions.

Machine learning techniques are also effective in mitigating NLOS errors [20-24], such as the semi-supervised learning approach proposed in [21] that uses self-training. Furthermore, deep learning and graph optimization techniques are utilized in [25, 26] to achieve ranging error mitigation.

After obtaining the required data from the signaling process for locating the target object, the positioning system needs mathematical processes to determine the target's position. Least-Squares (LS) [27, 28] and Extended Kalman Filter (EKF) [29] are two common methods used for estimating the position. LS is described in detail in [30]. This paper provides a comprehensive explanation of TWR algorithms, LS, and EKF methods in Part II, while the adapted tree approach and its description are presented in Part III. Part IV presents the results of applying the proposed approach, and finally, Part V concludes the paper.

The highlights of the paper compared to the existing literature are as follows:

I. Our study proposes a novel approach for mitigating ranging errors in UWB-based positioning systems using an adapted tree approach based on practical distance measurements.
II. The adapted tree approach is shown to significantly improve ranging accuracy, particularly in the presence of NLOS conditions, with an average error reduction of about 133 cm using the EKF estimation method.
III. Our approach is effective for both static and moving tags, demonstrating an accuracy of about 20.8 cm in LOS conditions and 24.1 cm in NLOS conditions through the EKF method.
IV. The study highlights the importance of considering LOS and NLOS conditions in UWB-based positioning systems and provides insights into the behavior of ranging errors in specific distance intervals.
V. Our findings have practical implications for various applications such as indoor localization, asset tracking, and unmanned aerial vehicle navigation.

II.PRELIMINARIES

Wireless signal-based positioning methodologies are typically categorized into ranging-based and non-ranging-based methods. The UWB positioning approach commonly employs a ranging-based algorithm, characterized by two sequential steps. The initial step involves the measurement of distance information, followed by the subsequent step wherein the positional coordinates are calculated utilizing the acquired distance information. TOF ranging emerges as a prevalent technique for measuring the distance between two nodes. In Section A, we delve into an examination of different TWR algorithms, elucidating their capacity to provide accurate TOF values. Meanwhile, Section B is dedicated to an extensive exposition of Position Estimation Methods derived from the measured distance information.

A. General study of TWR algorithms

TOF ranging algorithms play a crucial role in localization and tracking systems. TWR is one such algorithm that has gained prominence due to its capability to perform ranging without requiring the cores of modules to be synchronized. TWR can be classified into four methods [31], Single-Sided TWR (SS-TWR), Symmetric-Double-Sided TWR (SDS-TWR), Alternative-Double-Sided TWR (AltDS-TWR), and Asymmetric Double-Sided TWR (ADS-TWR).

1) Single-Sided TWR (SS-TWR):

In SS-TWR, two devices exchange signals to measure ToF. The signal round-trip starts when device A sends a signal at time τ_{ATx}, which reaches device B at time τ_{BRx}, after traveling for time T_{tof}. Once device B receives the signal, it sends back a response signal to device A with a specific delay t_{replyB}, which is shown as follows.

$$t_{replyB} = \tau_{BTx} - \tau_{BRx}. \quad (1)$$

The signal reaches device A at time τ_{ARx}. The time range from τ_{ATx} to τ_{ARx} is called t_{roundA} and its mathematical representation is given by (2).

$$t_{roundA} = 2T_{tof} + t_{replyB}. \quad (2)$$

The ToF, can be calculated as follows:

$$T_{tof} = \frac{1}{2}(t_{roundA} - t_{replyB}). \quad (3)$$

2) Symmetric-Double-Sided TWR (SDS-TWR):

SDS-TWR involves additional steps as compared to SS-TWR. After receiving the response signal from device B, device A waits for a period of time delay t_{replyA} before sending another signal to device B. The rest of the process is the same as SS-TWR, and the round-trip times for devices A and B are given by:

$$t_{roundA} = 2T_{tof} + t_{replyB},$$
$$t_{roundB} = 2T_{tof} + t_{replyA}. \quad (4)$$

To remember, t_{roundA} and t_{roundB} are the true times at devices A and B, respectively, in which the signal has taken to have a round-trip.

By combining the equations in (4), the formulation for T_{tof} is obtained as follows:

$$T_{tof} = \frac{1}{4}((t_{roundA} - t_{replyA}) + (t_{roundB} - t_{replyB})). \quad (5)$$

SDS-TWR takes longer than SS-TWR but has better accuracy. Illustrations of SS-TWR and SDS-TWR are available in Fig. 1.

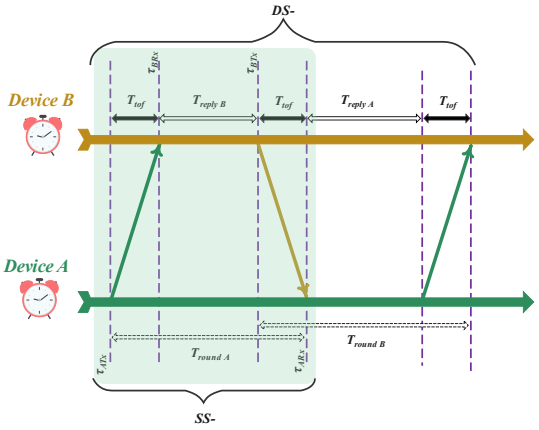

Fig. 1. Representation of Single- and Double-sided TWR methods.

3) Asymmetric Double-Sided TWR (ADS-TWR):

In ADS-TWR, device B does not need to send a response signal to device A. Therefore t_{replyA} is zero, and the round-trip time for device B is given by (7), while that for device A is given by (6). The ToF can be calculated using equation (8).

Fig. 2 illustrates how the ADS-TWR method plays its role.

$$t_{roundA} = 2T_{tof} + t_{replyB}, \quad (6)$$
$$t_{roundB} = 2T_{tof}, \quad (7)$$

$$T_{tof} = {}^{1}/_{4}((t_{roundA} + t_{roundB} - t_{replyB})). \quad (8)$$

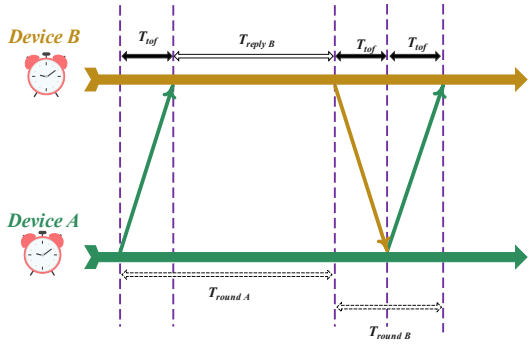

Fig. 2. Representation of Asymmetric Double-sided TWR method.

4) Alternative-Double-Sided TWR (AltDS-TWR):

AltDS-TWR has the same signaling process as SDS-TWR but uses a different mathematical approach. AltDS-TWR approach calculates the T_{tof} using the multiplication of (4) instead of their addition, as it is followed below:

$$t_{roundA} \times t_{roundB} = (2T_{tof} + t_{replyB}) \times (2T_{tof} + t_{replyA}). \quad (9)$$

Having simplified (9), the formulation for T_{tof} is achieved as:

$$T_{tof} = \frac{(t_{roundA}) \times (t_{roundB}) - (t_{replyA}) \times (t_{replyB})}{t_{roundA} + t_{roundB} + t_{replyA} + t_{replyB}}. \quad (10)$$

TWR methods face various errors, and comparison studies indicate that SDS-TWR and AltDS-TWR perform better than SS-TWR and ADS-TWR. Among the two, AltDS-TWR is superior to SDS-TWR due to better error minimization. Therefore, AltDS-TWR is chosen for practical tests.

B. Position estimation methods

Let T_{tof} represents the time of flight duration between the Tag and each individual Anchor in the context of a positioning system. After completing the ranging process, multilateration is used to determine the position of the tag relative to the distance between the tag and its surrounding anchors. The distance, d, can be calculated as:

$$d = c \times T_{tof}, \quad (11)$$

where c is the propagation velocity of electromagnetic waves. Trilateration results in a unique position as long as the three anchors are not in a straight line. Considering the unknown tag located at (x, y) and the i^{th} anchor located at (x_i, y_i), the actual distance between the tag and the i^{th} anchor, denoted as d_i, can be written as below:

$$d_i = \sqrt{(x - x_i)^2 + (y - y_i)^2}, i = 1,2,3,..,n. \quad (12)$$

presuming the existence of three anchors for positioning, each distance establishes an equation governing the position of the unknown tag as follows:

$$\begin{cases} {d_1}^2 = (x-x_1)^2 + (y-y_1)^2 \\ {d_2}^2 = (x-x_2)^2 + (y-y_2)^2 \\ {d_3}^2 = (x-x_3)^2 + (y-y_3)^2 \end{cases}. \quad (13)$$

Let d_i' denote the measured distance between the unknown tag and the i^{th} anchor. Then, the difference between the actual distance and the measured distance can be written as:

$$f_i(x,y) = d_i - d_i' = \sqrt{(x-x_i)^2 + (y-y_i)^2} - d_i' . \quad (14)$$

1) Linear and non-linear least squares methods:

To deal with the ranging noise, we adopt the LS method to minimize the summation value of all square errors as below:

$$F_i(x,y) = \sum_{i=1}^{n} (d_i - d_i')^2 = \sum_{i=1}^{n} {f_i}^2(x,y). \quad (15)$$

Let all equations in (13) subtract its first equation, we can get $A\varepsilon = b$, where $A = \begin{bmatrix} x_2 - x_1 & y_2 - y_1 \\ x_3 - x_1 & y_3 - y_1 \end{bmatrix}$, $\varepsilon = \begin{bmatrix} x \\ y \end{bmatrix}$, $b = \frac{1}{2}\begin{bmatrix} {x_2}^2 + {y_2}^2 - {d_2}^2 - ({x_1}^2 + {y_1}^2 - {d_1}^2) \\ {x_3}^2 + {y_3}^2 - {d_3}^2 - ({x_1}^2 + {y_1}^2 - {d_1}^2) \end{bmatrix}$, which is the linearized form of the LS. Thus, the Linear-LS (LLS) solution of ε is

$$\hat{\varepsilon} = (A^T A)^{-1} A^T b. \quad (16)$$

When the linearization is done, one measured range is lost, which is sometimes undesirable. As an alternative, Non-Linear Least Squares (NLLS) method is available, which does not include the mentioned linearization step. Newton's iterative method is a classical method for solving nonlinear equations. The basic idea is to make the nonlinear equations linearized and make the solution of linear equations approach the solution of nonlinear equations as close as possible.

Newton's iteration is used as the algorithm for minimizing the squared errors. The Jacobian in (17) for the set of equations is determined from partial differentiating (14) concerning x and y. The vectors f and r are introduced as:

$$J = 2\begin{bmatrix} \frac{\partial f_1}{\partial x} & \frac{\partial f_2}{\partial x} & \cdots & \frac{\partial f_n}{\partial x} \\ \frac{\partial f_1}{\partial y} & \frac{\partial f_2}{\partial y} & \cdots & \frac{\partial f_n}{\partial y} \end{bmatrix}^T, f = \begin{bmatrix} f_1 \\ f_2 \\ \vdots \\ f_n \end{bmatrix}, r = \begin{bmatrix} x \\ y \end{bmatrix}. \quad (17)$$

Newton's iteration gives, $r_{k+1} = r_k - (J_k^T J_k)^{-1} J_k^T f_k$, where r_{k+1} is the current position and r_k is the last approximated position. An estimated guess of the initial position can be obtained by using LLS. Since this is an iterative process, the algorithm will terminate when the difference between the k and $k+1$ iteration converges to an acceptable value.

2) Extended Kalman filter method:

The measurements in positioning are corrupted by noise. Therefore, EKF is the proper approach for this application [5]. The coordinates of the 2D position of the tag, $X = [x(k) \quad y(k)]^T$, where k refers to the sample time, are selected as the state variables of the filter. The state dynamics are modeled as follows:

$$X_k = F_k X_{k-1} + W_{k-1}, \quad (18)$$

where F_k denotes the state transition matrix, $W_{k-1} = [w_x(k-1) \quad w_y(k-1)]^T$ denotes process noise vector with zero mean and variance $E[{W_k}^T W_k] = Q_k$ at time k. The equation that relates the measurements to the state variables is $Z_k = h(X_k) + V_k$ where V_k is random measurement noise with variance $E[{V_k}^T V_k] = R_k$. In UWB positioning, the elements of the vector $h(X)$ are distances between the tag and neighbor anchors as follow:

$$h(X_k) = \begin{bmatrix} \sqrt{(x-x_1)^2 + (y-y_1)^2} \\ \sqrt{(x-x_2)^2 + (y-y_2)^2} \\ \sqrt{(x-x_3)^2 + (y-y_3)^2} \end{bmatrix}. \quad (19)$$

EKF algorithm can be used on linear systems. So (19) must be linearized for its nonlinearity. By taking the first-order Taylor expansion at each time step, the Jacobian matrix H_k, is obtained as follows:

$$H_k = \left[\frac{\partial h(X_k)}{\partial X_k}\right]_{X_k = \hat{X}_k} \quad (20)$$

In the prediction step (estimation equations), the prior estimated state can be expressed as:

$$\hat{X}_k^- = F\hat{X}_{k-1} \quad (21)$$

Here, the state vectors X, are the positions $x(k)$ and $y(k)$ at sample k. The state transition matrix F in (21) is time-invariant and is given as $F = \begin{bmatrix} 1 & 0 \\ 0 & 1 \end{bmatrix}$. Matrix F is the transition matrix that predicts the next state from the previous state, the current location of the tag is assumed to be the previous location. Here, we define a priori estimation error covariance P_k^- and a posteriori estimation error covariance P_k, which are subject to Gaussian noise:

$$P_k^- = FP_{k-1}F^T + Q_k. \quad (22)$$

The Kalman gain for measurement update is computed using the linearized H_k matrix, and the measurement updates of the state and the covariance are obtained as below:

$$K_k = P_k^- H_k^T (H_k P_k^- H_k^T + R_k)^{-1},$$
$$\hat{X}_k = \hat{X}_k^- + K_k\left(Z_k - h(\hat{X}_k^-)\right),$$
$$P_k = (I - K_k H_k)P_k^-, \quad (23)$$

where the predicted measurement is $\hat{Z}_k = h(\hat{X}_k^-)$. Z_k is the new sample mean of the distance measurements, R_k is the corresponding sample variance, and I is the identity matrix of order 2×2.

The filter has been initialized by setting $\hat{X}_0$ and P_0 to constant values. The first measurement update was evaluated iteratively, i.e., repeating the evaluation of (21) and (23) with the same measurement information until the predetermined convergence criterion is met.

To address the stability concern, consider the dynamic system (18) alongside the developed Kalman filter

algorithms (22) and (23). Based on the research conducted by Rief et al. [32], it is established that System (18) is exponentially bounded in mean square and bounded with probability one, provided certain conditions are met. Notably, the proposed method adheres to these conditions, which are outlined as follows:

I. There are positive real numbers $f, h, p1, p2, \hat{q}, \hat{r} > 0$ such that the following bounds are satisfied for every $k \geq 0$:

$$\|F_k\| \leq f, \|H_k\| \leq h, \quad (24)$$

$$p1I \leq P_k \leq p2I, \quad (25)$$

$$\hat{q}I \leq \hat{Q}_k, \quad \hat{r}I \leq \hat{R}_k . \quad (26)$$

II. F_k is non-singular for every $k \geq 0$.

III. There are positive real numbers $\varepsilon_\phi, \varepsilon_\chi, k_\phi, k_\chi > 0$ such that the functions ϕ and χ are bounded from above via:

$$\|\phi(y,z)\| \leq k_\phi \times \|x_k - m_k\|^2 , \quad (27)$$

$$\|\chi(y,z)\| \leq k_\chi \times \|x_k - m_k\|^2, \quad (28)$$

$$\|x_k - m_k\| \leq \varepsilon_\phi, \quad (29)$$

$$\|x_k - m_k\| \leq \varepsilon_\chi. \quad (30)$$

III. ADAPTED TREE APPROACH

Ranging data errors are a common occurrence, and clock drift is one type of error that is typically encountered. Due to real-world conditions, the clock cannot maintain a constant rate, resulting in clock drift. Other errors include Propagation Time Delay (PTD), Transmission Time Delay (TTD), Receiving Time Delay (RTD), and Preamble Accumulation Time Delay (PATD). PTD is caused by obstacles that delay the signal from the transmitter to the receiver, while TTD and RTD refer to the time taken by the transmitter and the receiver to create the signal message. Electronic components such as PCB and antenna also contribute to TTD and RTD. PATD is a delay caused by signal interference in a multipath situation [33].

A. Experimental methodology

The effectiveness of the adapted tree approach hinges upon rigorous experimental testing and precise measurement of ranging errors across varying distances between the tag and anchor. Accurate ranging errors are obtained through meticulous comparison of the measured distance between a tag and anchor with the actual distance. This disparity constitutes the ranging error, a crucial metric in assessing the performance of positioning systems.

Two distinct types of ranging errors commonly manifest: LOS and NLOS. LOS errors typically arise from factors such as clock drift, TTD, and RTD, while NLOS errors are compounded by PTD and PATD, alongside LOS error sources. In this section, we present an elaborate elucidation of both the experimental setup and the deployment of the Adapted Tree Approach, aimed at effectively mitigating ranging errors inherent in positioning systems.

1) Experimental setup:

The experiments were conducted using an UWB positioning system in a controlled laboratory environment. The UWB system comprised tags and anchors deployed within the test area. Tags transmitted signals, while anchors served as reference points for positioning based on the AltDS-TWR algorithm.

To simulate LOS and NLOS conditions, obstacles were strategically placed within the test environment. LOS conditions were ensured when the direct line of sight between the tag and anchor was unobstructed. To achieve this, we utilized a football stadium, providing ample space for unimpeded signal transmission. Conversely, NLOS conditions were induced by introducing obstacles that caused signal reflections and multipath effects. For this purpose, we utilized a laboratory setting equipped with tables, chairs, and common equipment found in typical laboratory environments. These obstructions replicated real-world scenarios where signal paths are obstructed, leading to NLOS conditions.

2) Data collection and error analysis:

Ranging data was collected by measuring the distance between tags and anchors using the UWB system. Each measurement cycle involved multiple iterations to ensure the reliability and accuracy of the measurements. Additionally, to enhance the robustness of the data collection process, two random devices were utilized to verify the validity of the results.

Following data collection, ranging errors underwent meticulous analysis to identify patterns and trends. This comprehensive analysis included computing both the mean error and standard deviation error for predefined distance intervals. By systematically examining the ranging errors across various distance intervals, valuable insights into the behavior and characteristics of the positioning system under different conditions were gained. This rigorous error analysis served as the foundation for evaluating the effectiveness of the adapted tree approach in mitigating ranging errors. Fig. 3 illustrates that ranging accuracy is significantly influenced by whether the measurement is conducted in LOS or NLOS conditions. To address these errors, the adapted tree approach is initiated.

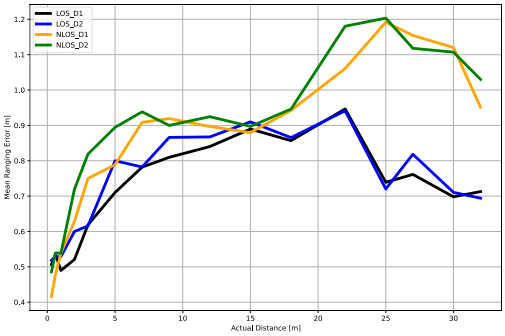

Fig. 3. Ranging Error relative to actual distance in the LOS and NLOS conditions for two measurements in both conditions.

B. Adapted tree approach:

The adapted tree approach was employed to mitigate ranging errors through interval-based error correction. Upon analyzing the ranging error values, it became evident that errors exhibited similar behavior within specific distance intervals, as demonstrated in Fig. 4 and Fig. 5 for LOS and NLOS conditions, respectively. To establish intervals, a maximum standard deviation error of 2.9 cm was utilized as a criterion. In both figures, the blue and red plots depict the behavior of the first and second devices, respectively, indicating consistent operation under each sight condition.

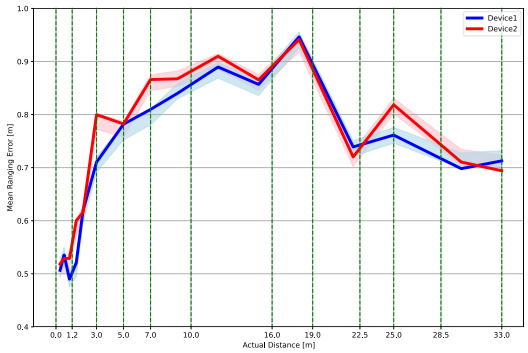

Fig. 4. Ranging Error relative to actual distance in the LOS condition for a couple of anchors.

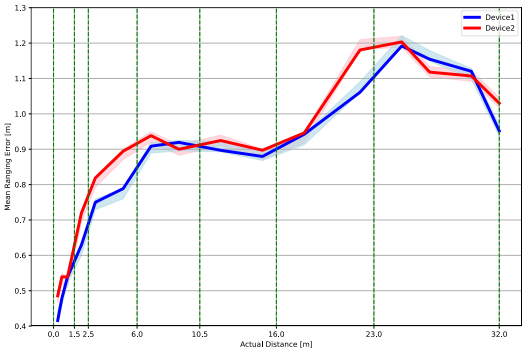

Fig. 5. Ranging Error relative to actual distance in the NLOS condition.

Intervals and their corresponding statistics are detailed in TABLE I and TABLE II for LOS and NLOS conditions, respectively. Furthermore, Fig. 6 and Fig. 7, presented on the following page, depict the data for each defined interval in LOS and NLOS conditions, respectively. Histograms associated with these intervals reveal a Gaussian distribution.

By subtracting adapted error values from the corresponding interval, notable enhancements in distance measurements were achieved. It is worth noting that since positioning relies on tag distances from anchors, mitigating distance errors inherently leads to mitigating positioning errors.

The simplicity, operational efficiency, and practicality of this method make it highly effective. Despite its simplicity, the adapted tree approach proves to be a robust and reliable solution for mitigating ranging errors in positioning systems.

TABLE I
LOS STATISTICS OF RANGING ERRORS

Interval [m]	Mean Error [m]	Standard Deviation (std) Error [m]
[0-1.2]	0.535	0.019
(1.2-2]	0.636	0.022
(2,3]	0.610	0.020
(3,5]	0.700	0.017
(5,7]	0.807	0.023
(7,10]	0.985	0.016
(10,16]	1.051	0.013
(16, 19]	1.090	0.027
(19, 22.5]	1.115	0.013
(22.5, 25]	0.990	0.029
(25, 28.5]	0.765	0.025
(28.5,33]	0.589	0.029

TABLE II
NLOS STATISTICS OF RANGING ERRORS

Interval [m]	Mean Error [m]	Standard Deviation (std) Error [m]
[0-1.5]	0.589	0.020
(1.5-2.5]	0.695	0.022
(2.5,6]	0.820	0.020
(6,10.5]	0.940	0.018
(10.5,16]	1.015	0.019
(16,23]	1.105	0.016
(23, 32]	1.185	0.014

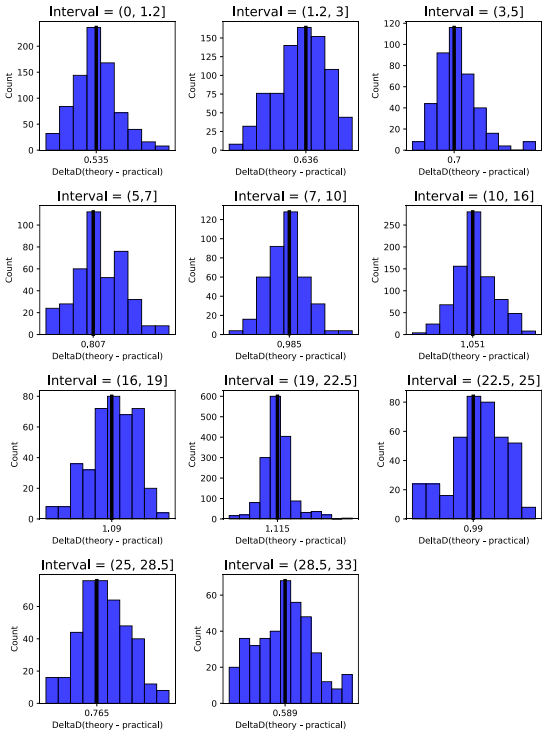

Fig. 6. LOS intervals data histograms

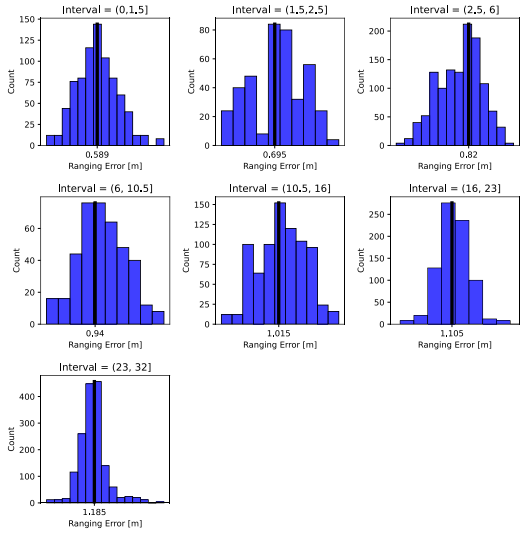

Fig. 7. NLOS intervals data histograms

IV.POSITIONING RESULTS

In this section, we provide a detailed discussion of our positioning results. Our team conducted tests using modular boards that incorporated an ATmega32U4-AU micro-controller, Decawave DWM1000 module, and ESP8266 SMT Module - ESP-12E, as illustrated in Fig. 8.

We conducted tests in both LOS and NLOS environments at the Iran University of Science and Technology football stadium and the Advanced Instrumentation Laboratory of the Electrical Engineering School, as shown in Fig. 9 and Fig. 10, respectively. Each test utilized four modules as anchors and one module as the tag, with the AltDS-TWR time-based algorithm used for all tests. We utilized the LLS, NLLS, and EKF estimators, which were introduced in Section 2, to estimate the tag's position.

Since accurate error analysis is not feasible for the moving tag, we conducted positioning error analysis tests on fixed points in two dimensions, X and Y. For this purpose, positioning experiments were carried out at six fixed points in both LOS and NLOS conditions. In LOS conditions, the fixed points were located at coordinates [2,3], [4,13.5], [8,0], [0,4.95], [10.1,6.95], and [14.3,1]. Similarly, for NLOS conditions, the fixed points were positioned at coordinates [1.45,4], [4.6,0], [4.65,2.3], [6.65,0.48], [10.05,4.8], and [12.43,2.32].

Subsequent to data collection, positioning error analysis was performed. The results, comparing the positioning error with and without utilizing the adapted tree for each estimator, are presented in TABLE III and TABLE IV for LOS and NLOS conditions respectively.

Fig. 8. Developed RTLS board.

Fig. 9. LOS condition positioning environment.

Fig. 10. NLOS condition positioning environment.

TABLE III
POSITIONING ERRORS OF DIFFERENT METHODS IN LOS CONDITION

Actual Position [m]		Positioning Method Errors [m]					
		LLS		NLLS		EKF	
X	Y	Simple	Adapted	Simple	Adapted	Simple	Adapted
2	3	0.621	0.233	0.595	0.239	0.556	0.167
4	13.5	0.447	0.435	0.873	0.450	0.963	0.438
8	0	0.592	0.157	1.096	0.195	1.125	0.224
8	4.95	0.324	0.168	0.446	0.172	0.232	0.092
10.1	6.95	0.241	0.184	0.363	0.058	0.351	0.062
14.3	1	0.824	0.243	1.205	0.265	1.223	0.263

TABLE IV
POSITIONING ERRORS OF DIFFERENT METHODS IN NLOS CONDITION

Actual Position [m]		Positioning Method Errors [m]					
		LLS		NLLS		EKF	
X	Y	Simple	Adapted	Simple	Adapted	Simple	Adapted
1.45	4	0.925	0.485	1.692	0.301	1.713	0.292
4.6	0	0.394	0.189	1.564	0.179	1.556	0.177
4.65	2.3	0.353	0.252	1.599	0.278	1.649	0.268
6.65	0.48	0.433	0.287	1.419	0.330	1.463	0.317
10.05	4.8	0.715	0.167	1.510	0.121	1.533	0.121
12.43	2.32	1.391	0.456	1.438	0.299	1.506	0.270

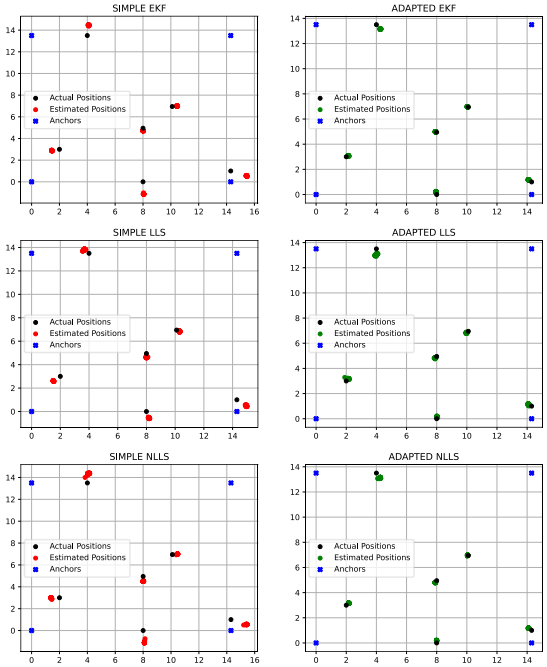

Fig. 11. Positioning in LOS condition. Left: without Adapted Tree / Right: with Adapted Tree.

To further illustrate the effectiveness of the adapted tree method, Fig. 11 and Fig. 12 show the error mitigation in the LOS and NLOS conditions, respectively. The results indicate that both the NLLS and EKF estimation methods have higher accuracy than the LLS method. Furthermore, a comparison of the accuracy of the EKF and NLLS estimators in Fig. 13 shows that the EKF is the more accurate estimator, despite their similar accuracy levels.

Additionally, the Root Mean Square Error (RMSE) for the said points in LOS and NLOS conditions is visualized in Fig. 14 and Fig. 15, providing further insights into the performance of the adapted tree approach across different estimators and environmental conditions.

Upon analyzing the results, it was found that utilizing the adapted tree leads to significant error mitigation. Specifically, in the LOS condition, the average error reduction is 53.4 cm, 27.2 cm, and 53.2 cm with the EKF, LLS, and NLLS methods respectively. In the NLOS condition, the adapted tree results in an average error reduction of about 132.9 cm, 39.5 cm, and 128.5 cm with EKF, LLS, and NLLS respectively.

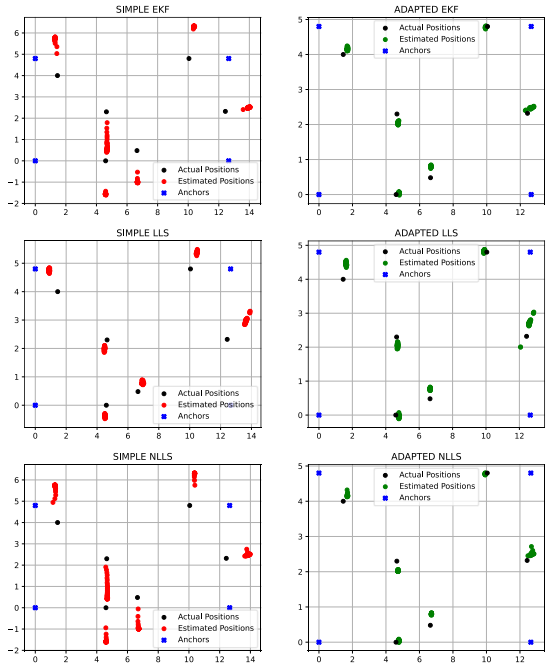

Fig. 12. Positioning in NLOS condition. Left: without Adapted Tree / Right: with Adapted Tree

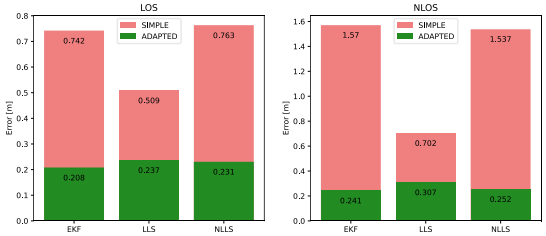

Fig. 13. Average positioning errors for each method in LOS and NLOS conditions [m].

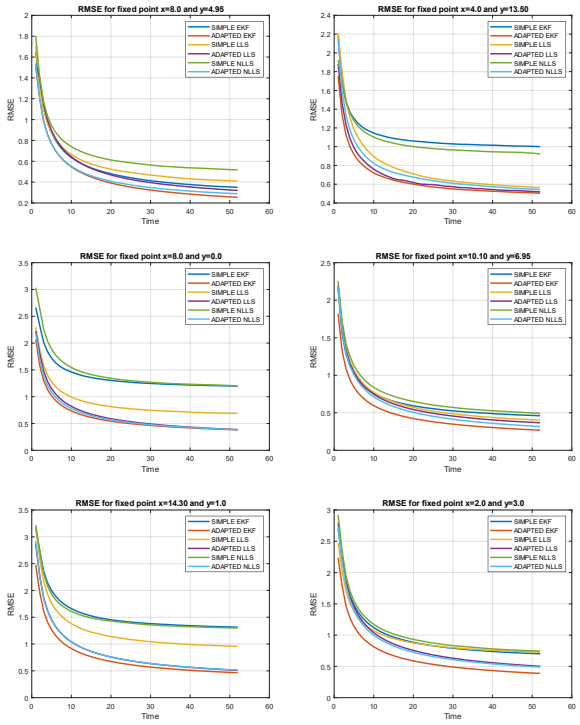

Fig. 14. RMSE analysis for fixed points in LOS conditions, comparing positioning error with and without utilizing the adapted tree approach for each estimator. 'SIMPLE' prefix before the estimators denotes no use of adapted tree approach, while 'ADAPTED' prefix signifies its utilization.

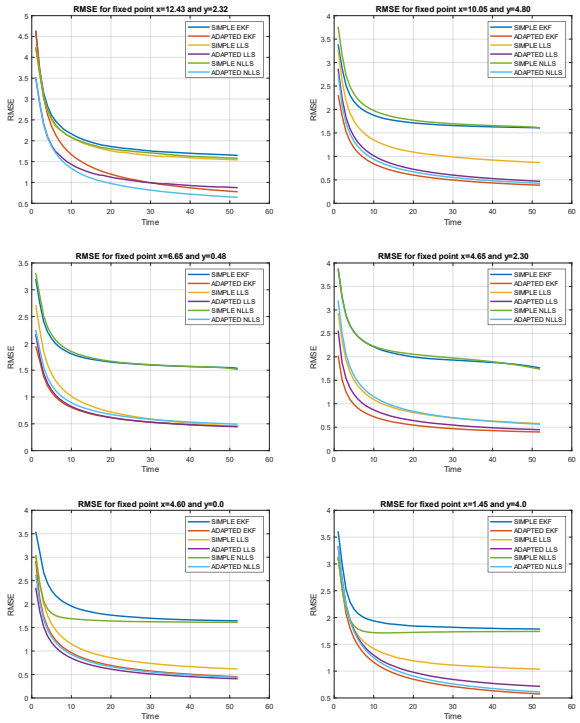

Fig. 15. RMSE analysis for fixed points in NLOS conditions, comparing positioning error with and without utilizing the adapted tree approach for each estimator. 'SIMPLE' prefix before the estimators denotes no use of adapted tree approach, while 'ADAPTED' prefix signifies its utilization.

In addition, Fig. 16 and Fig. 17 demonstrate the application of our proposed approach on a moving tag, showing its effectiveness in both LOS and NLOS conditions. Our approach has achieved an accuracy of about 20.8 cm for LOS and 24.1 cm for NLOS conditions through the EKF method. In a broader context, when compared to existing literature, our method exhibits notable accuracy. The precision achieved in this paper surpasses that of [34] by 66.8% and exceeds [35] by 16.7%, underscoring the superior performance of our proposed approach.

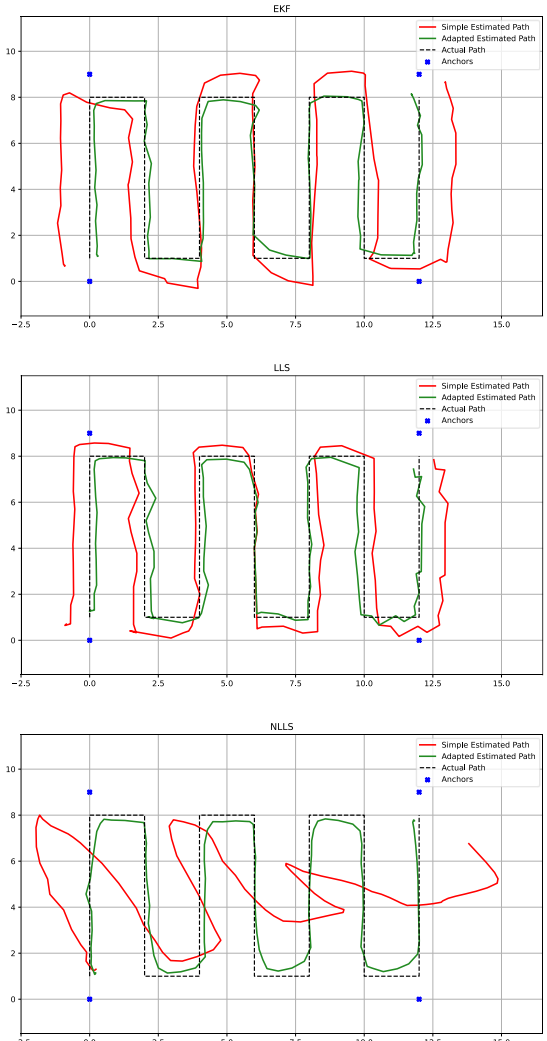

Fig. 16. Positioning of a moving object in LOS conditions. Blue dots represent anchor locations, and the black dashed line shows the true trajectory. The green path is the trajectory estimated with the EKF combined with the proposed method (adapted tree), while the red path is solely estimated by EKF without the proposed method. 'Simple' prefix before the estimated path denotes no use of adapted tree approach, while 'Adapted' prefix signifies its utilization.

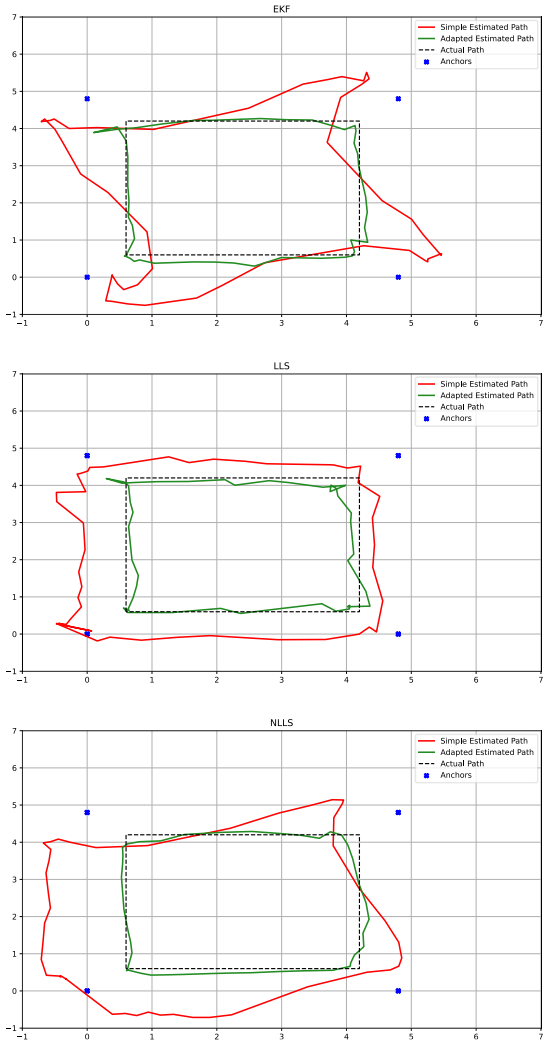

Fig. 17. Positioning of a moving object in NLOS conditions. Blue dots represent anchor locations, and the black dashed line shows the true trajectory. The green path is the trajectory estimated with the EKF combined with the proposed method (adapted tree), while the red path is solely estimated by EKF without the proposed method. 'Simple' prefix before the estimated path denotes no use of adapted tree approach, while 'Adapted' prefix signifies its utilization.

V. Conclusion

This paper has investigated the challenge of error mitigation in UWB-based positioning systems, offering a novel approach grounded in practical distance measurements. Our findings underscore the inevitable nature of ranging errors within such systems, necessitating robust mitigation strategies.

The introduced adapted tree approach serves as a promising solution to address these errors, leveraging insights gleaned from rigorous experimentation. Our analysis reveals a profound dependency of ranging accuracy on the presence of LOS and NLOS conditions, highlighting the critical importance of environmental factors.

Through comprehensive testing, we have demonstrated the significant efficacy of the adapted tree approach in mitigating ranging errors. Notably, our results indicate an average error reduction of approximately 53.4 cm in LOS conditions and about 133 cm in NLOS conditions, with the EKF estimation method exhibiting superior accuracy. Moreover, our approach proves effective even in scenarios involving a moving tag, showcasing its versatility and applicability across diverse conditions. The achieved accuracy levels in both LOS and NLOS conditions surpass existing benchmarks in the literature, emphasizing the practical significance of our proposed method.

Acknowledgment

The authors would like to express their gratitude to the Iran National Science Foundation (INSF) for providing financial support and necessary facilities to carry out this research, under Project No. 98026676. Special thanks also go to Mr. Alireza Mohammadi Hamed for his invaluable contribution in the development of the hardware used in this study.

References

[1] A. Sharif *et al.*, "Compact base station antenna based on image theory for UWB/5G RTLS embraced smart parking of driverless cars," *IEEE Access*, vol. 7, pp. 180898-180909, 2019.

[2] A. R. J. Ruiz and F. S. Granja, "Comparing ubisense, bespoon, and decawave uwb location systems: Indoor performance analysis," *IEEE Transactions on instrumentation and Measurement*, vol. 66, no. 8, pp. 2106-2117, 2017.

[3] F. Mazhar, M. G. Khan, and B. Sällberg, "Precise Indoor Positioning Using UWB: A Review of Methods, Algorithms and Implementations," *Wireless Personal Communications*, vol. 97, no. 3, pp. 4467-4491, 2017, doi: 10.1007/s11277-017-4734-x.

[4] H. J. Kim, Y. Xie, H. Yang, C. Lee, and T. L. Song, "An Efficient Indoor Target Tracking Algorithm Using TDOA Measurements With Applications to Ultra-Wideband Systems," *IEEE Access*, vol. 7, pp. 91435-91445, 2019.

[5] C. Zhou, J. Yuan, H. Liu, and J. Qiu, "Bluetooth indoor positioning based on RSSI and Kalman filter," *Wireless Personal Communications*, vol. 96, no. 3, pp. 4115-4130, 2017.

[6] C. Suwatthikul, W. Chantaweesomboon, S. Manatrinon, K. Athikulwongse, and K. Kaemarungsi, "Implication of anchor placement on performance of UWB real-time locating system," in *2017 8th International Conference of Information and Communication Technology for Embedded Systems (IC-ICTES)*, 2017: IEEE, pp. 1-6.

[7] S. Bottigliero, D. Milanesio, M. Saccani, and R. Maggiora, "A Low-Cost Indoor Real-Time Locating System Based on TDOA Estimation of UWB Pulse Sequences," *IEEE Transactions on Instrumentation and Measurement*, vol. 70, pp. 1-11, 2021.

[8] D. Feng, C. Wang, C. He, Y. Zhuang, and X.-G. Xia, "Kalman-Filter-Based Integration of IMU and UWB for High-Accuracy Indoor Positioning and Navigation," *IEEE Internet of Things Journal*, vol. 7, no. 4, pp. 3133-3146, 2020, doi: 10.1109/jiot.2020.2965115.

[9] X. Zhu, J. Yi, J. Cheng, and L. He, "Adapted error map based mobile robot UWB indoor positioning," *IEEE Transactions on Instrumentation and Measurement*, vol. 69, no. 9, pp. 6336-6350, 2020.

[10] C. Lian Sang, M. Adams, T. Hörmann, M. Hesse, M. Porrmann, and U. Rückert, "Numerical and experimental evaluation of error estimation for two-way ranging methods," *Sensors*, vol. 19, no. 3, p. 616, 2019.
[11] F. Despaux, A. Van den Bossche, K. Jaffrès-Runser, and T. Val, "N-TWR: An accurate time-of-flight-based N-ary ranging protocol for Ultra-Wide band," *Ad Hoc Networks*, vol. 79, pp. 1-19, 2018.
[12] J. Khodjaev, Y. Park, and A. Saeed Malik, "Survey of NLOS identification and error mitigation problems in UWB-based positioning algorithms for dense environments," *annals of telecommunications-annales des télécommunications*, vol. 65, no. 5, pp. 301-311, 2010.
[13] X. Yang, J. Wang, D. Song, B. Feng, and H. Ye, "A Novel NLOS Error Compensation Method Based IMU for UWB Indoor Positioning System," *IEEE Sensors Journal*, vol. 21, no. 9, pp. 11203-11212, 2021, doi: 10.1109/jsen.2021.3061468.
[14] D.-H. Kim, A. Farhad, and J.-Y. Pyun, "UWB positioning system based on LSTM classification with mitigated NLOS effects," *IEEE Internet of Things Journal*, 2022.
[15] Y. Huang, S. Mazuelas, F. Ge, and Y. Shen, "Indoor Localization System with NLOS Mitigation Based on Self-Training," *IEEE Transactions on Mobile Computing*, 2022.
[16] L. Barbieri, M. Brambilla, A. Trabattoni, S. Mervic, and M. Nicoli, "UWB localization in a smart factory: augmentation methods and experimental assessment," *IEEE Transactions on Instrumentation and Measurement*, vol. 70, pp. 1-18, 2021.
[17] B. Silva and G. P. Hancke, "Ranging error mitigation for through-the-wall non-line-of-sight conditions," *IEEE Transactions on Industrial Informatics*, vol. 16, no. 11, pp. 6903-6911, 2020.
[18] B. Cao, S. Wang, S. Ge, and W. Liu, "Improving the Positioning Accuracy of UWB System for Complicated Underground NLOS Environments," *IEEE Systems Journal*, 2021.
[19] S. Djosic, I. Stojanovic, M. Jovanovic, and G. L. Djordjevic, "Multi-algorithm UWB-based localization method for mixed LOS/NLOS environments," *Computer Communications*, vol. 181, pp. 365-373, 2022.
[20] V. Barral, C. J. Escudero, J. A. García-Naya, and R. Maneiro-Catoira, "NLOS identification and mitigation using low-cost UWB devices," *Sensors*, vol. 19, no. 16, p. 3464, 2019.
[21] T. Wang, K. Hu, Z. Li, K. Lin, J. Wang, and Y. Shen, "A semi-supervised learning approach for UWB ranging error mitigation," *IEEE Wireless Communications Letters*, vol. 10, no. 3, pp. 688-691, 2020.
[22] M. Hassan, N. Babaei, S. Ebadollahi, and B. Gill, "Database Optimization of Fingerprint-Based Indoor Positioning System Using Genetic Algorithm," in *2021 IEEE 12th Annual Information Technology, Electronics and Mobile Communication Conference (IEMCON)*, 2021: IEEE, pp. 0052-0057.
[23] J. Wei, H. Wang, S. Su, Y. Tang, X. Guo, and X. Sun, "NLOS identification using parallel deep learning model and time-frequency information in UWB-based positioning system," *Measurement*, vol. 195, p. 111191, 2022.
[24] M. Malajner, D. Gleich, and P. Planinsic, "Soil type characterization for moisture estimation using machine learning and UWB-Time of Flight measurements," *Measurement*, vol. 146, pp. 537-543, 2019.
[25] S. Angarano, V. Mazzia, F. Salvetti, G. Fantin, and M. Chiaberge, "Robust ultra-wideband range error mitigation with deep learning at the edge," *Engineering Applications of Artificial Intelligence*, vol. 102, p. 104278, 2021.
[26] S. Zheng *et al.*, "Multi-robot relative positioning and orientation system based on UWB range and graph optimization," *Measurement*, vol. 195, p. 111068, 2022.
[27] J. Yan, C. C. Tiberius, G. J. Janssen, P. J. Teunissen, and G. Bellusci, "Review of range-based positioning algorithms," *IEEE Aerospace and Electronic Systems Magazine*, vol. 28, no. 8, pp. 2-27, 2013.
[28] A. Yassin *et al.*, "Recent advances in indoor localization: A survey on theoretical approaches and applications," *IEEE Communications Surveys & Tutorials*, vol. 19, no. 2, pp. 1327-1346, 2016.
[29] F. Deng, H.-L. Yang, and L.-J. Wang, "Adaptive unscented Kalman filter based estimation and filtering for dynamic positioning with model uncertainties," *International Journal of Control, Automation and Systems*, vol. 17, no. 3, pp. 667-678, 2019.
[30] J. Yan, "Algorithms for indoor positioning systems using ultra-wideband signals," 2010.
[31] I. Domuta and T. P. Palade, "Two-way ranging algorithms for clock error compensation," *IEEE Transactions on Vehicular Technology*, vol. 70, no. 8, pp. 8237-8250, 2021.
[32] K. Reif, S. Gunther, E. Yaz, and R. Unbehauen, "Stochastic stability of the discrete-time extended Kalman filter," *IEEE Transactions on Automatic control*, vol. 44, no. 4, pp. 714-728, 1999.
[33] J. Cano, G. Pagès, E. Chaumette, and J. LeNy, "Clock and power-induced bias correction for UWB time-of-flight measurements," *IEEE Robotics and Automation Letters*, vol. 7, no. 2, pp. 2431-2438, 2022.
[34] Y. Wang and X. Li, "The IMU/UWB Fusion Positioning Algorithm Based on a Particle Filter," *ISPRS International Journal of Geo-Information*, vol. 6, no. 8, 2017, doi: 10.3390/ijgi6080235.
[35] S. Sung, H. Kim, and J.-I. Jung, "Accurate Indoor Positioning for UWB-Based Personal Devices Using Deep Learning," *IEEE Access*, vol. 11, pp. 20095-20113, 2023.